Ferroelectrics

ISSN: 0015-0193 (Print) 1563-5112 (Online) Journal homepage: https://www.tandfonline.com/loi/gfer20

Design of the transducer for multi-direction wind energy harvesting based on PZT

Xiaohua Zhou, Jiaheng Zou, Diyuan Gan, Xin Gou, Yuda Chen, Ruyun Tian & Tongjian Guo

To cite this article: Xiaohua Zhou, Jiaheng Zou, Diyuan Gan, Xin Gou, Yuda Chen, Ruyun Tian & Tongjian Guo (2019) Design of the transducer for multi-direction wind energy harvesting based on PZT, Ferroelectrics, 550:1, 196-209, DOI: 10.1080/00150193.2019.1652508

To link to this article: https://doi.org/10.1080/00150193.2019.1652508

Published online: 31 Oct 2019.

FERROELECTRICS
2019, VOL. 550, 196–209
https://doi.org/10.1080/00150193.2019.1652508

Design of the transducer for multi-direction wind energy harvesting based on PZT

Xiaohua Zhou[a], Jiaheng Zou[a], Diyuan Gan[a], Xin Gou[c], Yuda Chen[a], Ruyun Tian[a], and Tongjian Guo[b]

[a]College of Instrumentation and Electrical Engineering, Jilin University, Changchun, China; [b]Changchun Institute of Optics, Fine Mechanics and Physics, Chinese Academy of Sciences, Changchun, China; [c]State Key Laboratory of Power Transmission Equipment & System Security and New Technology, Chongqing University, Chongqing, China

ABSTRACT
This paper presents key design ideas and performance of the transducer for multi-direction wind energy harvesting. Lead zirconate titanate (PZT) and cantilever beam are introduced to set up the piezoelectric vibrator unit for vibration-to-electric energy conversion. The conversion circuit and the storage unit are designed to output and store electric energy. In addition, wireless data transmission system based on microprocessor is proposed to realize information acquisition for data acquisition nodes. The experimental results show that the transducer achieves good practical property, and it can fill a 25 mAh lithium polymer battery with the continuous 40 min work in the 11 m s^{-1} wind speed environment. The transducer can work without the wind direction restrictions. It can be widely used in data monitoring, wireless data transmission and other fields with simple structure, high energy utilization rate, low cost and environmental-friendly.

ARTICLE HISTORY
Received 17 March 2018
Accepted 11 June 2019

KEYWORDS
Multi-direction wind energy harvesting; PZT (lead zirconate titanate); cantilever beam; conversion circuit; wireless data transmission

1. Introduction

Nowadays, the application of micro-power equipment is becoming more and more widespread, but its long time power supply problem is caused, such as data acquisition and monitoring equipment for long time work in the outdoor. Since the capacity of the battery is limited, and it is impossible to replace the battery, many efforts have been made to find out the energy harvesting technology as a self-power source. The researchers are generally favored in the ubiquitous solar energy, thermal energy and vibration energy in the natural environment [1]. However, it should be noticed that solar energy, thermal energy and vibration energy is not the best choice for its limit seasons and regions. On the contrary, wind energy is a kind of renewable energy with high energy density in the environment. It can combine well with other energy sources to form the benign complement. Accordingly, the wind energy transducer becomes one of the most attractive options for harvesting wind energy.

CONTACT Tongjian Guo tjguo_ciomp@aliyun.com
Color versions of one or more of the figures in the article can be found online at www.tandfonline.com/gfer.

Transducer for wind energy harvesting can convert the wind energy into vibration mechanical energy, and then convert the mechanical energy into electric energy through electromagnetic, electrostatic or piezoelectric devices [2]. Electromagnetic vibration energy harvesting is to generate electric current in the coil by relative motion between the coil and magnetic field with vibration. It has low conversion efficiency, large volume and high cost. The electrostatic vibration energy harvesting is composed of two capacitor plates. It can realize vibration-to-electric energy conversion by overcome static electric power between the capacitors using the external vibration. Compared with the same size electromagnetic vibration energy harvesting, the electrostatic vibration energy harvesting can obtain higher output voltage. However, in order to realize the charge constraint or voltage constraint at both ends of the capacitor, additional starting voltage source support is required, which greatly restrict the independence application on network nodes.

Lead zirconate titanate (PZT) is a kind of electronic ceramic material with piezoelectric properties. It can convert mechanical energy and electric energy with each other. It has been widely used in medical imaging, acoustic sensors, acoustic transducers, ultrasonic motors and other fields [3].The piezoelectric transducer for wind energy harvesting can to convert external vibration into electric energy based on positive piezoelectric effect of the piezoelectric material [4]. It has many advantages. Piezoelectric material has high energy density, and the piezoelectric transducer for wind energy harvesting can produce high output power with small deformation. Compared with electromagnetic vibration energy harvesting, the piezoelectric transducer for wind energy harvesting is easy to miniaturize with simple structure. Compared with electrostatic vibration energy harvesting, the piezoelectric transducer for wind energy harvesting need not additional voltage source, which guarantees energy recovery independence.

We have designed and implemented the transducer for multi-direction wind energy harvesting based on PZT. It has a high utilization rate of wind energy in all directions without alignment the wind direction. The key issues have been analyzed and designed such as piezoelectric vibrator unit, mechanical structure of the transducer, circuit system and application system. A good application effect is presented.

2. Electroceramic properties of PZT

PZT is the ceramic perovskite material that shows the marked piezoelectric effect. Positive piezoelectric effect is caused by external forces, resulting in changes in the electric field within the material, which will release the charge on the surface of the material [5]. Being piezoelectric, PZT develops a voltage across two of its faces when compressed. Since the external vibration energy can be converted into electrical energy, PZT is suitable for fabrication of the wind energy harvesting.

The piezoelectric material used in energy collection should have different performance requirements under different conditions. In order to meet the requirements of wind energy harvesting, high energy density piezoelectric material is chosen. Since most piezoelectric energy harvesting is generally targeted at the vibration energy and the vibration frequency below 150 Hz in the natural environment, the piezoelectric energy harvesting at the low frequency is given priority to discussion here.

The piezoelectric chip in a natural state (low frequency) can be considered as a capacitor. The electric energy U generated under alternating stress can be expressed as follows:

$$U = \frac{1}{2} C V^2 \tag{1}$$

where C is capacitance and V is the open circuit voltage.

The open circuit voltage in Equation (1) can be expressed as follows:

$$V = -gX \cdot t \tag{2}$$

where g is the voltage constant, X is stress and t is thickness.

The capacitance C in Equation (1) can be expressed as follows:

$$C = \frac{\varepsilon \cdot A}{t} \tag{3}$$

where ε is the free permittivity and A is the effective area of the sample.

In addition, the relationship between the strain constant d and the voltage constant g can be expressed as follows:

$$d = g \cdot \varepsilon \tag{4}$$

So Equation (1) can be simplified as follows:

$$U = \frac{1}{2}(d \cdot g) \cdot X^2 \cdot A \cdot t \tag{5}$$

where $A \cdot t$ is the volume of the material.

So the energy under per unit volume (energy density) can be expressed as follows:

$$u = \frac{1}{2}(d \cdot g) \cdot X^2 \tag{6}$$

It can be seen from Equation (6) that X is determined according to the experimental condition and d and g are related to the material. The energy density of the material can be characterized by the strain constant d of the piezoelectric material and the voltage constant g.

Therefore, the piezoelectric material with high piezoelectric coefficient d should be chosen to improve the vibration-to-electric energy conversion efficiency of the transducer and high voltage constant g allows the vibration to generate high voltage at the same excitation to increase the power output efficiency of the transducer.

3. Mechanical system designs

The mechanical system is one of the important parts of the transducer, and its structure directly affects the energy conversion efficiency of the transducer. The mechanical system is mainly composed of piezoelectric vibrator unit and wind energy collection chamber. The piezoelectric vibrator unit is the key to the vibration-to-electric conversion by the positive piezoelectric effect [6]. The wind energy collection chamber is used to collect wind energy in the environment to improve the efficiency of vibration-to-electric energy conversion.

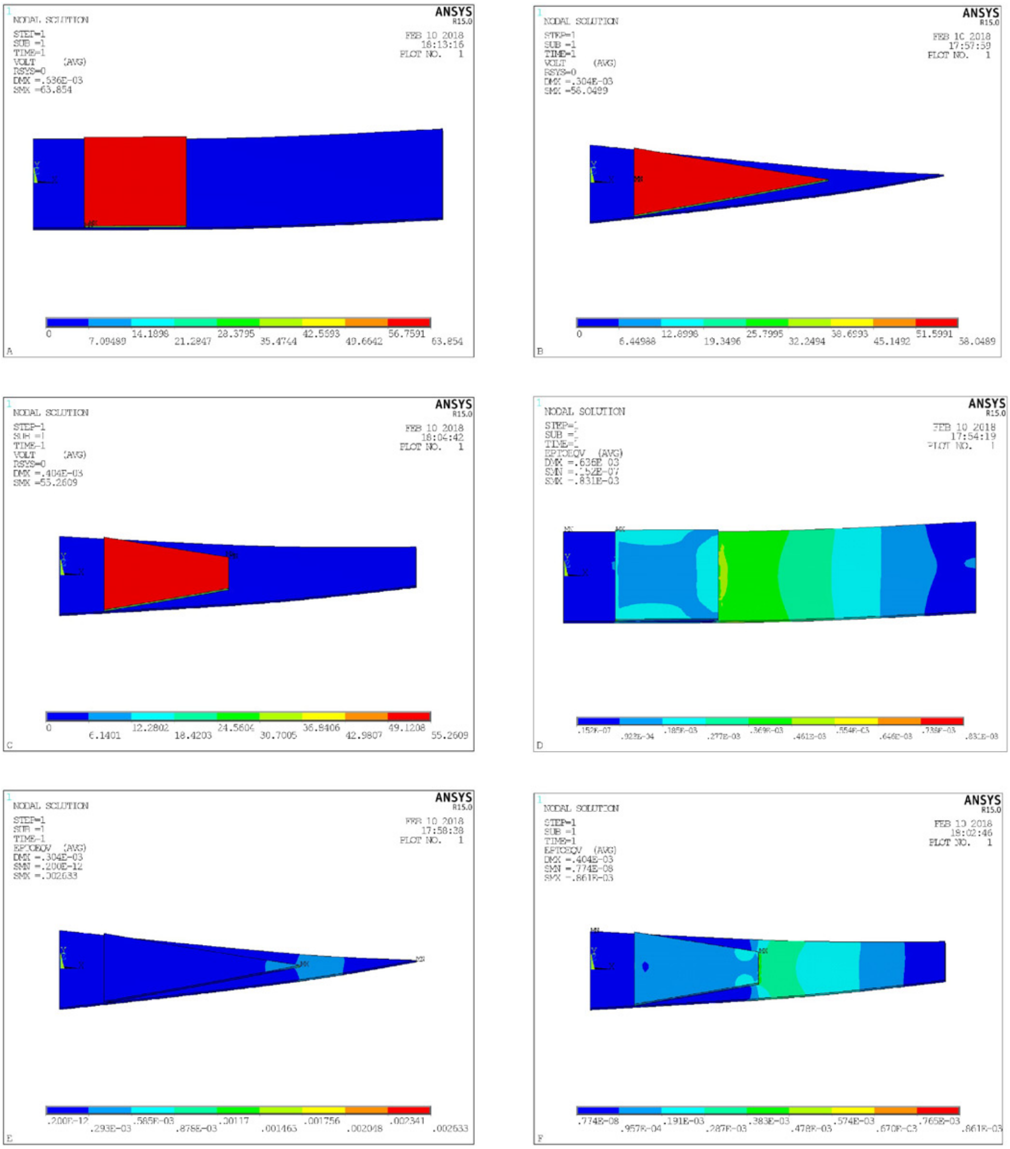

Figure 1. (A) Voltage cloud map of rectangular piezoelectric vibrator unit. (B) Voltage cloud map of triangular piezoelectric vibrator unit. (C) Voltage cloud map of trapezoidal piezoelectric vibrator unit. (D) Strain cloud map of rectangular piezoelectric vibrator unit. (E) Strain cloud map of triangular piezoelectric vibrator unit. (F) Strain cloud map of trapezoidal piezoelectric vibrator unit.

3.1. Piezoelectric vibrator unit

The electric dipole moment in the piezoelectric material changes when the piezoelectric material is subjected to physical stress or strain. At the same time, the piezoelectric material produces an equal amount of positive and negative charge on the relative surface of the material to resist the change [7]. Piezoelectric ceramics are of high hardness and brittleness, which can produce little displacement and deformation. So they are seldom

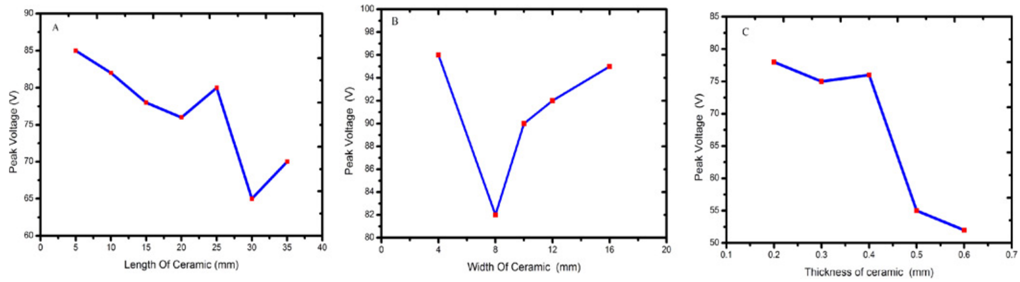

Figure 2. (A) Output peak voltage of the different length ceramic flakes. (B) Output peak voltage of the different width ceramic flakes. (C) Output peak voltage of the different thickness ceramic flakes.

used alone. To overcome this problem, we put the piezoelectric ceramics and elastomers stick together to form a composite piezoelectric vibrator unit.

In order to improve the power output efficiency of the transducer, we use the piezoelectric system with high piezoelectric coefficient and high electromechanical coupling coefficient. The piezoelectric material suitable for elastic modulus is chosen to prevent from cracking under external forces. The piezoelectric ceramic material with low dielectric and mechanical loss is used to avoid reducing mechanical energy due to the loss of piezoelectric ceramic material. Based on the transducer demand analysis of piezoelectric materials, PZN and PNN are brought into the PZT binary system to form the piezoelectric material of the quaternary system, which is called PZT–PZN–PNN [8]. The $d \cdot g$ numerical value of 0.8PZT–0.1PZN–0.1PNN is $20019 \times 10^{-15} \mathrm{m}^2/\mathrm{N}$, which is high $d \cdot g$ numerical value in the system. This can meet the performance requirements of piezoelectric material in the transducer.

As for the support mode of the piezoelectric vibrator, the piezoelectric cantilever beam has the largest deflection and the lowest resonant frequency among the rigid support mode, the free-free boundary support mode and the simple support mode. It is easy to simplify the structure of the transducer [9]. Therefore, the piezoelectric cantilever beam is used as support mode of piezoelectric vibrator unit to improve the energy conversion efficiency of the transducer, which is conducive to the reliability operation and long service life of the device.

In order to select the appropriate shape of the piezoelectric vibrator unit, the voltage and strain output of different piezoelectric vibrator units are simulated by ANSYS software. The piezoelectric vibrator units are supported by the cantilever beam. Their shapes are rectangular, triangular and trapezoidal. The three types of piezoelectric vibrators have the same thickness and surface area with the same thickness, length and width of the copper. The voltage cloud map and strain cloud map of different piezoelectric vibrator units are shown in Figure 1.

The rectangular piezoelectric vibrator has the highest output voltage under the same force in Figure 1(A–C). The rectangular piezoelectric vibrator has the least strain in Figure 1(D–F). Since piezoelectric ceramic is brittle, it is better to extend the life of the piezoelectric vibrator unit with less deformation in the higher output voltage. Therefore, we adopt the rectangular piezoelectric vibrator unit with high output voltage and less deformation relatively in other piezoelectric vibrator units.

The influence of different sizes of ceramic and copper flakes on the output voltage is analyzed. When the size of the copper flake is $40 \times 10 \times 0.4$mm, the length, width and

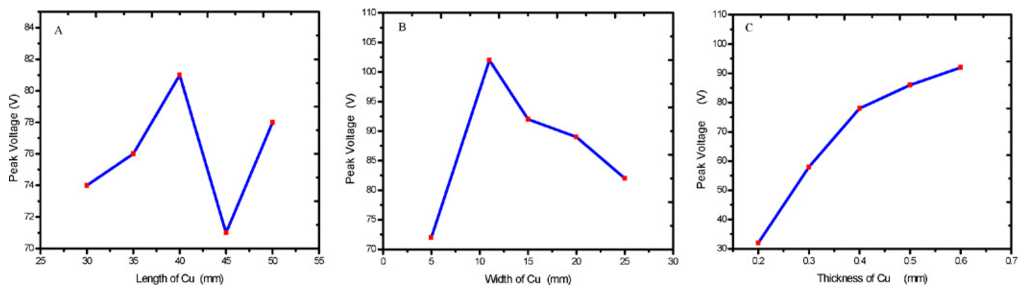

Figure 3. (A) Output peak voltage of the different length copper flakes. (B) Output peak voltage of the different width copper flakes. (C) Output peak voltage of the different thickness copper flakes.

thickness of the piezoelectric ceramic are different. The output peak voltage is shown in Figure 2. When the size of piezoelectric ceramics is $10 \times 10 \times 0.4$mm, the length, width and thickness of the copper flake are different. The output peak voltage is shown in Figure 3.

The width and thickness of the piezoelectric ceramic flake is 10×0.4mm in Figure 2. The output voltage of the ceramic flake at less than 25 mm length is relatively stable. In other words, the length has little influence. But it dropped suddenly at 30 mm. This is because the length of the ceramic flake is already three-fourths length of the substrate. The stiffness of the piezoelectric vibrator increases and the vibration decreases. When the length and thickness of the piezoelectric ceramic is 10×0.4mm and the width of ceramic flake is from 4 to 8 mm, the output voltage decreases as the width increases. When the width of ceramic flake is 10 mm, which is the same as that of copper flake, output voltage rises slightly. When the length and width of the piezoelectric ceramic is 10×10mm, the thickness of the ceramic flake is 0.4mm, the output voltage increases obviously. However, the overall output voltage decreases with the increase of thickness, and the variation range is not large.

The width and thickness of the copper flake is 10×0.4mm in Figure 3. The output peak voltage of the copper flake has a peak at 40 mm length and it reaches the lowest point at 45 mm length. Then the peak voltage increases with the increasing length of the copper flake. In other words, stiffness affects the vibration of ceramic flake. When the length and thickness of the copper flake is 40×0.4mm, the output peak voltage of the copper flake has a maximum value at 11 mm width and then it goes down. When the length and width of the copper flake is 40×10mm, the output peak voltage is positively correlated with the thickness. This means that the thickness of copper flake has important influence on the output voltage in a certain range.

To sum up, we choose the piezoelectric material of PZN and PNN introduced in the PZT binary system (PZT–PZN–PNN). The piezoelectric cantilever beam is used as the support mode of the rectangular piezoelectric vibrator unit. The effective length, width and thickness of the piezoelectric ceramic flake is $10 \times 10 \times 0.4$mm. The effective length, width and thickness of the copper flake is $40 \times 10 \times 0.4$mm.

3.2. Wind energy collection chamber

Wind energy collection chamber is mainly used to collect wind energy in the environment to improve the utilization rate of wind energy. The shell is the main body part of wind

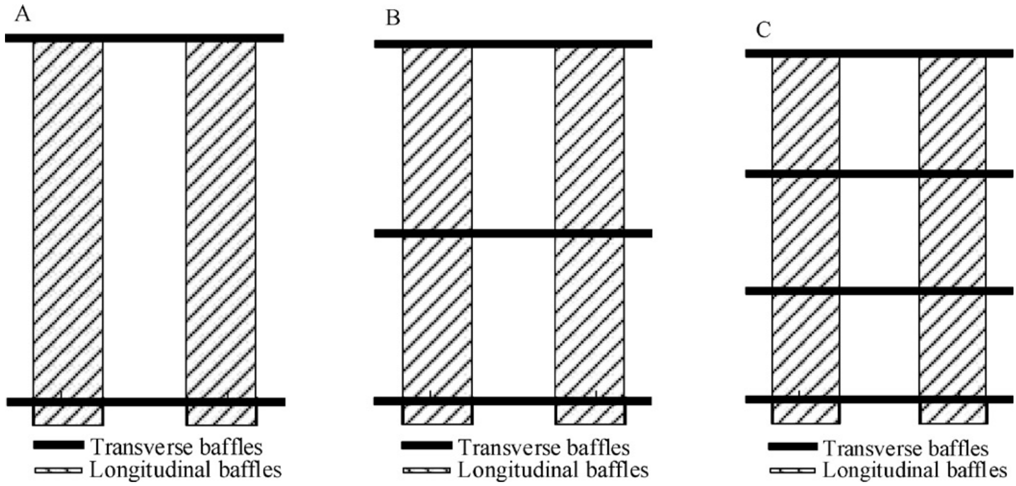

Figure 4. (A) Front view of the shell with two transverse baffles and four longitudinal baffles. (B) Front view of the shell with three transverse baffles and four longitudinal baffles. (C) Front view of the shell with four transverse baffles and four longitudinal baffles.

energy collection chamber. It is assembled for the connection, support, fixation and protection, and restraining the wind flow. The shell is cylindrical and divided by transverse and longitudinal baffles. The transverse and longitudinal baffles are vertically intersected and interlocked each other. The wind energy collection chamber is divided into different fan-shaped units.

In order to optimize the shell structure of the energy collection chamber and improve the efficiency of vibration-to-electric energy conversion, the output power of the shell composed of the different baffles are compared and analyzed. When two, three and four transverse baffles are vertically intersected with four, six and eight longitudinal baffles, the wind energy collection chamber is divided into different fan-shaped units. The schematic of different structural forms of the shell is in Figures 4 and 5. The output power of the wind energy harvester when connected with a resistance of 20KΩ is in Figure 6.

The output power of wind energy harvester with the different shell structure increases when the wind speed increases in Figure 6. As the wind speed is less than $14\mathrm{m}\cdot\mathrm{s}^{-1}$, the greater number of transverse baffles, the more output energy in Figure 6(A). However, the output energy decreases in the form of the four transverse baffles when the wind speed increases. This is because the space of every fan-shaped unit reduces when many fan-shaped units are divided by the great number of baffles, which is not conducive to the wind flow. Thus the vibration performance of the piezoelectric vibrator unit has been influenced. As the wind speed is less than 8 m/s, the greater number of longitudinal baffles, the more output energy in Figure 6(B). However, as the wind speed increases, the output energy decreases in the more longitudinal baffles. This also verifies the reason described above.

On the whole, the output energy between the three and four transverse baffles is not much different, and the little different output energy among the four, six and eight longitudinal baffles. Taking into account the size, cost and practicality of the harvester, the output energy of the harvester with the three transverse baffles and the four longitudinal

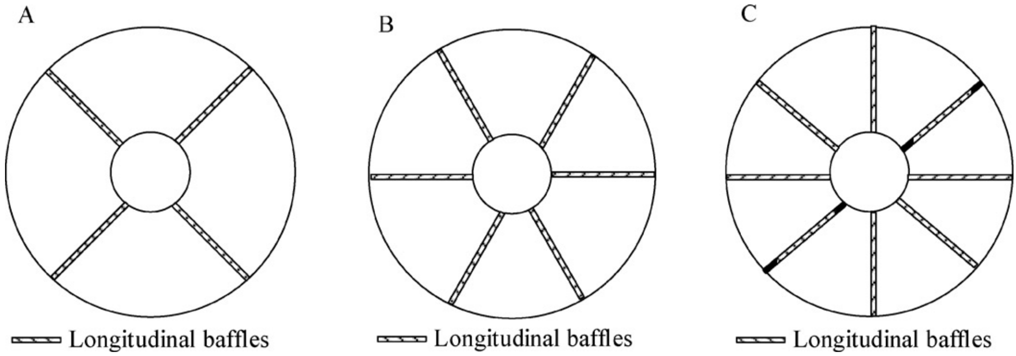

Figure 5. (A) Top view of the shell with three transverse baffles and four longitudinal baffles. (B) Top view of the shell with three transverse baffles and six longitudinal baffles. (C) Top view of the shell with three transverse baffles and eight longitudinal baffles.

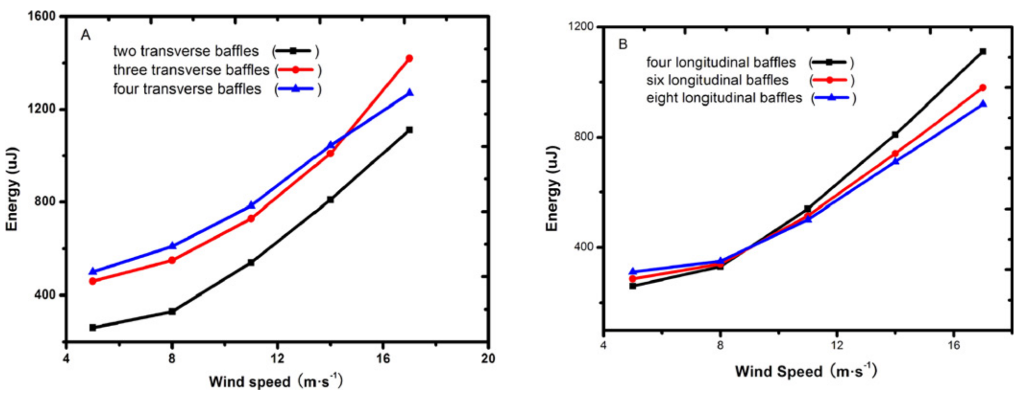

Figure 6. Output power of the wind energy harvester with different shell.

baffles has good stability and its performance can meet the demand. Therefore, the structure of the wind energy collection chamber is designed with three circular plate-shaped transverse baffles and four rectangular plate-shaped longitudinal baffles vertically staggered. The entire cylindrical wind energy collection chamber is divided into eight fan-shaped units. The same eight piezoelectric cantilever beam arrays are distributed around the eight fan-shaped units. Every piezoelectric cantilever beam array consists of five piezoelectric cantilevers. The two piezoelectric cantilevers are arranged in parallel on the upper and lower. The only one is on the middle. Wind energy collection chamber structure is shown in Figure 7.

4. Circuit system designs

The function of circuit system is to convert the non-regular alternating current (AC) generated by piezoelectric cantilever beam into direct current (DC), which can be utilized by low-power equipment. The circuit system consists of the rectification, parallel buffer, DC–DC boost convert and power management. The main components and circuit diagram of circuit system are shown in Figures 8 and 9.

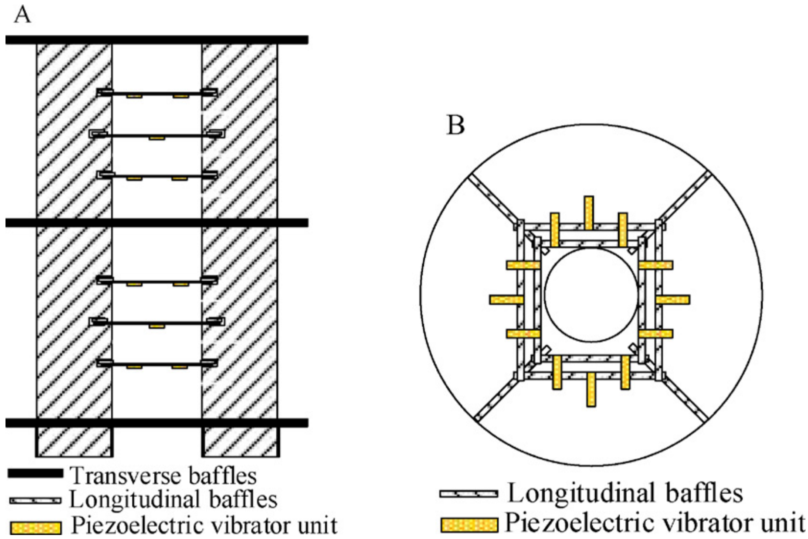

Figure 7. (A) Front view of the wind energy collection chamber. (B) Top view of the wind energy collection chamber.

4.1. Voltage-multiplying rectifying and poly flow buffer

Half-wave, full-wave, bridge type and voltage multiplying are the common rectifying schemes [10]. The voltage doubling rectifier is chosen because the output voltage amplitude of piezoelectric cantilever beam is small. The node voltage drop of voltage doubling rectifier circuit is smaller than others. The diode used in the circuit is the SD103AWS Schottky diode. Its positive voltage drop is only 0.4 V. It can effectively reduce the loss of rectifier circuit. Every piezoelectric cantilever beam is connected to one voltage doubling rectifier circuit. The generated non-regular AC voltage is converted into DC voltage.

Considering the limited current output capacity of a single piezoelectric cantilever beam, it is difficult to reach the minimum requirement for the follow-up processing circuit. Therefore, all the output current of the piezoelectric cantilever beam array in a fan-shaped unit is collected to the super capacitor. When electric energy accumulated in the super capacitor reaches the starting voltage of the subsequent circuit, the circuit is driven to run. The output of the voltage doubling rectifier circuit is connected to the super capacitor through the diode, which can effectively prevent the accumulated charge in the super capacitor from conversing to the voltage doubling rectifier circuit.

4.2. DC–DC boost and power management

When the circuit is working, the voltage of the super capacitor is lower than the supply voltage required by the general electronic system. Therefore, the DC–DC boost circuit is used to lift the low voltage to a higher DC voltage. The MAX1678 chip is a high-efficiency and low-noise DC–DC boost converter. Its starting voltage is reduced to 0.87 V voltage and the static working current is only 37 μA, which meets the requirement of low power loss [11]. In addition, MAX1678 has fixed voltage and two adjustable output

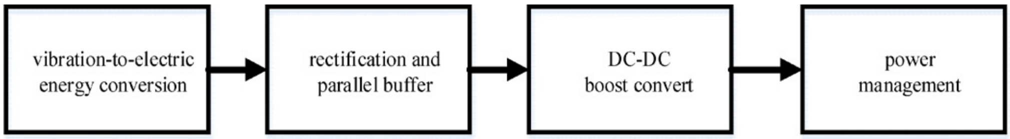

Figure 8. Main components of the circuit system.

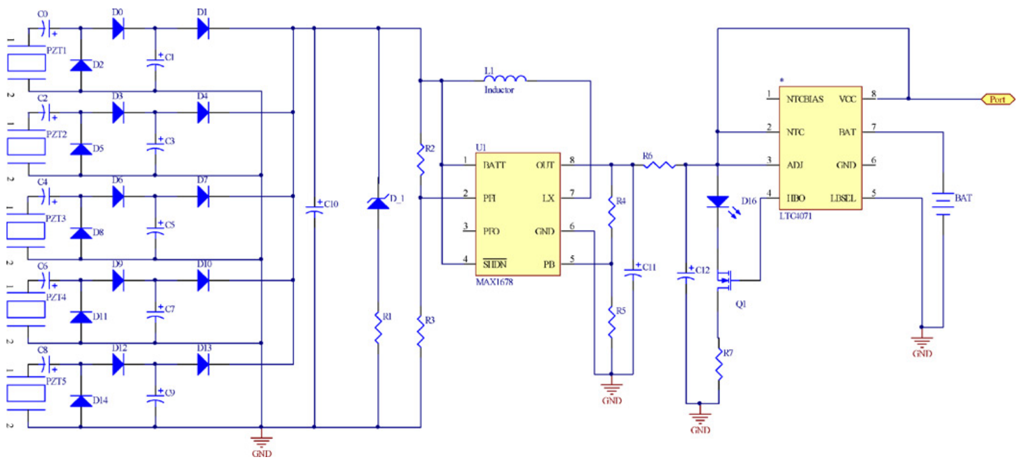

Figure 9. Main circuit diagram of the circuit system.

modes, which can help to meet the different application requirements of the circuit. This DC–DC boost circuit is based on the MAX1678 chip, and the output voltage is regulated by adjusting the resistance of the sampling resistor R_4 and R_5. At the same time, the effective input voltage of the booster circuit is regulated by adjusting the resistance of the sampling resistor R_2 and R_3. Because of the input limit voltage of MAX1678, the parallel Zener diode 1N4734 is connected between the super capacitor and the DC-DC boost circuit to ensure the safe and reliable operation of the circuit. This effectively prevents the super capacitor from overvoltage in a long continuous charging state.

In order to effectively store the energy collected from the eight fan-shaped units to the lithium polymer battery and avoid the over-charge and over-discharge of the battery, it is necessary to introduce the power management. The LTC4071 chip is capable of intermittent or continuous charging of the battery, and it can provide the selection of three kinds of suspension voltage [12]. In addition, the chip has a low battery power cutoff function, which can effectively prevent the lithium battery from being damaged by over-discharge.

5. Application system designs

The transducer for multi-direction wind energy harvesting can supply power to the wireless data transmission system to realize the self-supply of the data acquisition node. The wireless data transmission system consists of multiple data acquisition nodes and a base station. They communicate with each other to form a network. The system composed of the single data acquisition node and a base station is described as an example. The structure block diagram of the application system is shown in Figure 10.

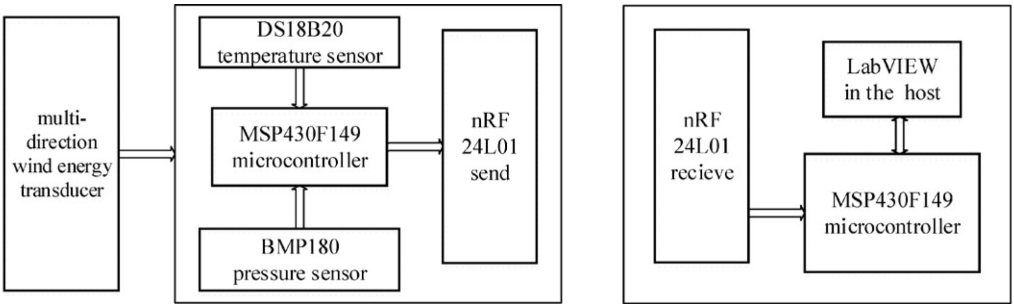

Figure 10. Structure block diagram of application system.

5.1. Data acquisition node

The data acquisition node is composed of MSP430F149 microcontroller, DS18B20 temperature sensor, BMP180 pressure sensor and nRF24L01 wireless module. The MSP430F149 microcontroller continuously reads the real time data from the pressure and temperature sensors. The collected data is sent to nRF24L01 after verification and processing inside the microprocessor to meet the communication requirements. Finally, the collected data is transmitted to the surrounding space via the nRF24L01 wireless data transmission module for the base station to obtain data.

5.2. Data receiving node

The data receiving node is also the base station of the whole application system. It is responsible for collecting the information from the subordinate data collection nodes and transferring them to the switchboard. The base station also selects MSP430F149 microcontroller as the main control chip. The interrupt working mode is used to real time read the information obtained by nRF24L01. The microcontroller collates the data, and then communicates with the host computer developed by LABVIEW software via the UART serial port. The whole system's data packet is transmitted to the host computer for display and storage, so as to prepare for subsequent data analysis and process.

6. Measurement of the transducer

The designed multi-direction wind energy transducer includes the shell, piezoelectric cantilever beam, energy conversion circuit and energy storage unit. The shell is cut and assembled from plexi-glass. It mainly plays a role in restraining the fluid. The piezoelectric cantilever beam is arranged in the shell. It converts the mechanical energy produced by wind vibration into the electric energy. The conversion circuit converts the non-regular AC from the piezoelectric cantilever beam to the stable DC by the rectifier and the voltage stabilizer, and finally the energy storage unit is used to store the electric energy generated by the whole transducer. It can also power the micro-power load. This transducer can collect multi-direction wind, so it has high utilization rate of wind energy. The prototype of the transducer is shown in Figure 11.

In order to analyze the energy conversion efficiency of the transducer, the test system is built with AFB0612EHE axial fan, AS836 digital speed detector, GDS-2202A digital

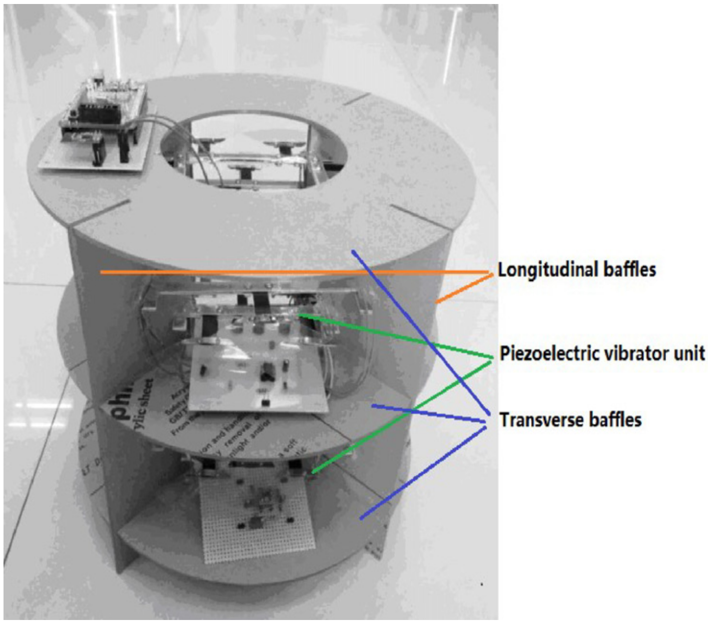

Figure 11. Prototype of the transducer.

oscilloscope, etc. The output voltage peak values with different resistors in 11 m/s wind speed is shown in Figure 12. The output power with different resistors in different wind speeds is shown in Figure 13.

As a whole, the output power increases with the increasing wind speed in Figure 13. The output power increases gradually when the resistance is below 50 KΩ. However, it decreases when the resistance is greater than 50 KΩ. That is, the loading capacity declines at this time.

To further test the application function of the transducer, the 25 mAh battery can be filled under the 40min continuous working of the transducer. At the same time, data acquisition nodes work normally when the lithium battery and data acquisition nodes are connected, and the laboratory temperature and pressure value can be sent to the host computer to monitor the work of the transducer.

7. Conclusions

A transducer utilizing PZT for multi-direction wind energy harvesting is designed, and simulated analyses and experimental measurements were presented to show the possible application of this transducer. The transducer consists of the shell, piezoelectric cantilever beam, energy conversion circuit and energy storage unit. Through detailed comparison and analysis, the rectangular piezoelectric vibrator unit composed of piezoelectric materials of the quaternary system is introduced. The piezoelectric cantilever beam as the support mode of the piezoelectric vibrator unit is put to use. The shell is designed with three circular plate-shaped transverse baffles and four rectangular plate-shaped longitudinal baffles vertically staggered. The output power performance of the wind energy is good. The energy conversion circuit and the storage unit are

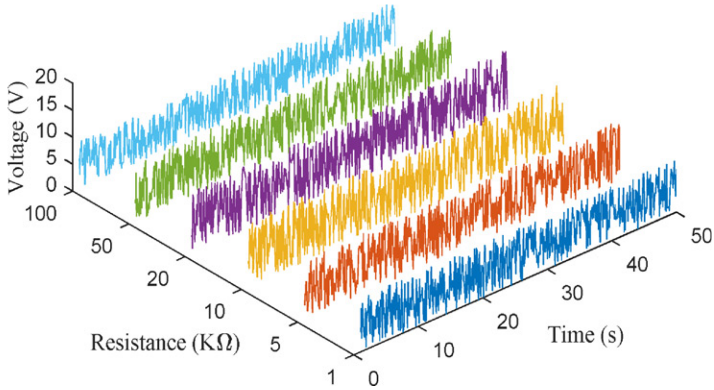

Figure 12. Voltage peak change with different resistors.

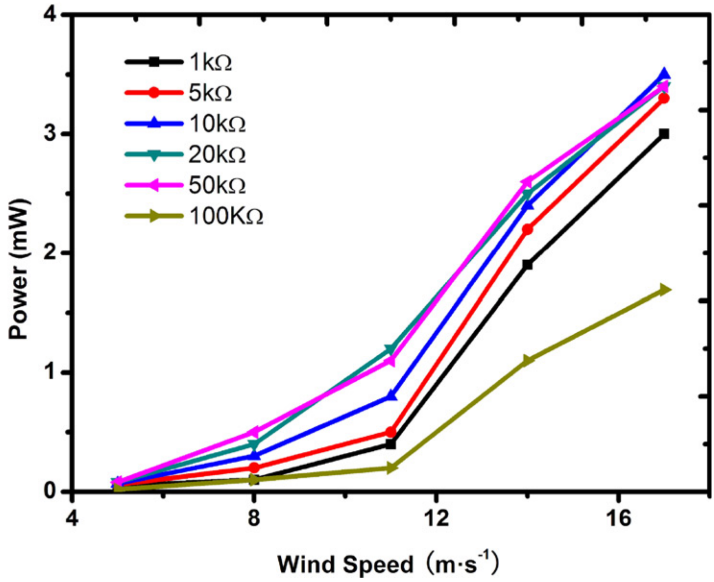

Figure 13. Output power with different resistors in different wind speeds.

designed with voltage-multiplying rectification, parallel buffer, DC-DC boost convert and storage unit. The output and storage of electric energy are completed. In addition, the proposed wireless data transmission system realizes the self-sufficiency of data acquisition nodes. Finally, the energy collection and loading capacity of the transducer are estimated through measured data, which proves its feasibility.

Several important notes for the application of the transducer were included. Firstly, the transducer can collect multi-direction wind energy without having to think about the wind direction. Therefore, it has high utilization rate of wind energy. Secondly, this transducer is simple in structure and environment-friendly, and it can be used outdoors for a long time. Thirdly, the data packet of the whole system can be transmitted to the host computer for display and storage, which can be applied to data collection and detection in the field. Finally, the transducer systems will find adaptations soon, although most experiments took place indoors. Advances in piezoelectric materials, preparation technology of piezoelectric cantilever beam and wireless data transmission technology will make the transducer more and more suitable for micro-power supply.

Acknowledgments

Authors express their gratitude to Changchun Institute of Optics, Fine Mechanics and Physics in Chinese Academy of Sciences and State Key Laboratory of Power Transmission Equipment and System Security and New Technology in Chongqing University for their generously provided experimental equipments. Authors would also like to thank anonymous reviewers provided many helpful comments on the manuscript.

Funding

This work was supported by the he National Natural Science Foundation of China under Grant 41204069; and New Energy Special Project of Jilin Province-University Construction Special Project under Grant SXGJSF2017-5. Any opinions, findings, conclusions and recommendations expressed in this paper are those of the authors.

References

[1] T. Dittrich, A. Belaidi, and A. Ennaoui, Concepts of inorganic solid-state nanostructured solar cells, *Solar Energ. Mater. Solar Cells* **95** (6), 1527–1536 (2011). DOI: 10.1016/j.solmat.2010.12.034.

[2] X. Zhuo *et al.*, Research progress on micro vibration energy harvesters, *Transducer Microsyst. Technol.* **34** (2), 9–12 (2015).

[3] L. X. Juan *et al.*, New headways and new applications of piezoceramics at home and abroad, *Bull. Chin. Ceram. Soc.* **25** (4), 101–107 (2006).

[4] B. Y. Xing *et al.*, Triboelectric nanogenerator tree for harvesting wind energy and illuminating in subway tunnel, *Adv. Mater. Technol.* **3** (3), 1700317 (2018). DOI: 10.1002/admt.201700317.

[5] A. Kumar *et al.*, Deformation induced electromagnetic response of soft and hard PZT under impact loading, *Ferroelectrics* **510** (1), 170–183 (2017). DOI: 10.1080/00150193.2017.1328726.

[6] S. M. Krishnasamy and T. R. Lenka, Distributed parameter modeling for autonomous charge extraction of various multilevel segmented piezoelectric energy harvesters, *Microsyst. Technol.* **24** (3), 1577–1587 (2018). DOI: 10.1007/s00542-017-3559-6.

[7] M. Kratzer *et al.*, Reconstruction of the domain orientation distribution function of polycrystalline PZT ceramics using vector piezoresponse force microscopy, *Sci. Rep.* **8** (1), 422 (2018). DOI: 10.1038/s41598-017-18843-4.

[8] S. Chandarak *et al.*, Structural investigation of PZT–PNN and PZT–PZN probed by synchrotron X-ray absorption spectroscopy, *Ferroelectrics* **455** (1), 117–122 (2013). DOI: 10.1080/00150193.2013.845485.

[9] R. Hosseini *et al.*, Parameter identification of partially covered piezoelectric cantilever power scavenger based on the coupled distributed parameter solution, *Int. J. Smart Nano Mater.* **8** (2–3), 110–124 (2017). DOI: 10.1080/19475411.2017.1343754.

[10] K. V. Cartwright and E. J. Kaminsky, New equations for capacitance vs ripple in power supplies, *Lat. Am. J. Phys. Educ.* **11** (1), 1301_01–1301_11 (2017).

[11] A. Singh, A. Goel, and A. Agarwal, A digital-based low-power fully differential comparator, *J. Circuits Syst. Comput.* **26** (1), 1051–1061 (2017).

[12] A. Costanzo *et al.*, Electromagnetic energy harvesting and wireless power transmission: a unified approach, *Proc. IEEE* **102** (11), 1692–1711 (2014).